- Board of Editors
- Publication Ethics
- Instructions to Author
- Plagiarism Policy
- Ethics Policy
- Track your Article
- Count Your API
- Post Publication
- Submit Article

Review of Research
ISSN No. : 2249-894X
Open Access
Monthly Publish
Save Tree, Save Paper, Save World

d in Qualis Capes / BRAZIL as B3

- Call for Book Chapters LBP ORJI Indexed new!
- Call for Book Reviews and Reviewers new!

Review of Research Journal is a Online International multidisciplinary research journal, published monthly in English, Hindi & Marathi Language. All research papers submitted to the journal will be double - blind peer reviewed referred by members of the editorial Board readers will include investigator in universities, research institutes government and industry with research interest in the general subjects.

Chief Editor

Ashok Yakkaldevi

Publication Place

Yakkaldevi,
Ravivar peth, Solapur
2011@gmail.com

Co-ordinator
IQAC
Shri Guru Buddhiswami Mahavidyalaya
Purna (Jn) Dist. Parbhani - 431511 (M.S.)

Estd. 1983

PRINCIPAL
Shri Guru Buddhiswami Mahavidyalaya
Purna (Jn.) Dist. Parbhani

IMG-20191205-WA0008.jpg (480×800)

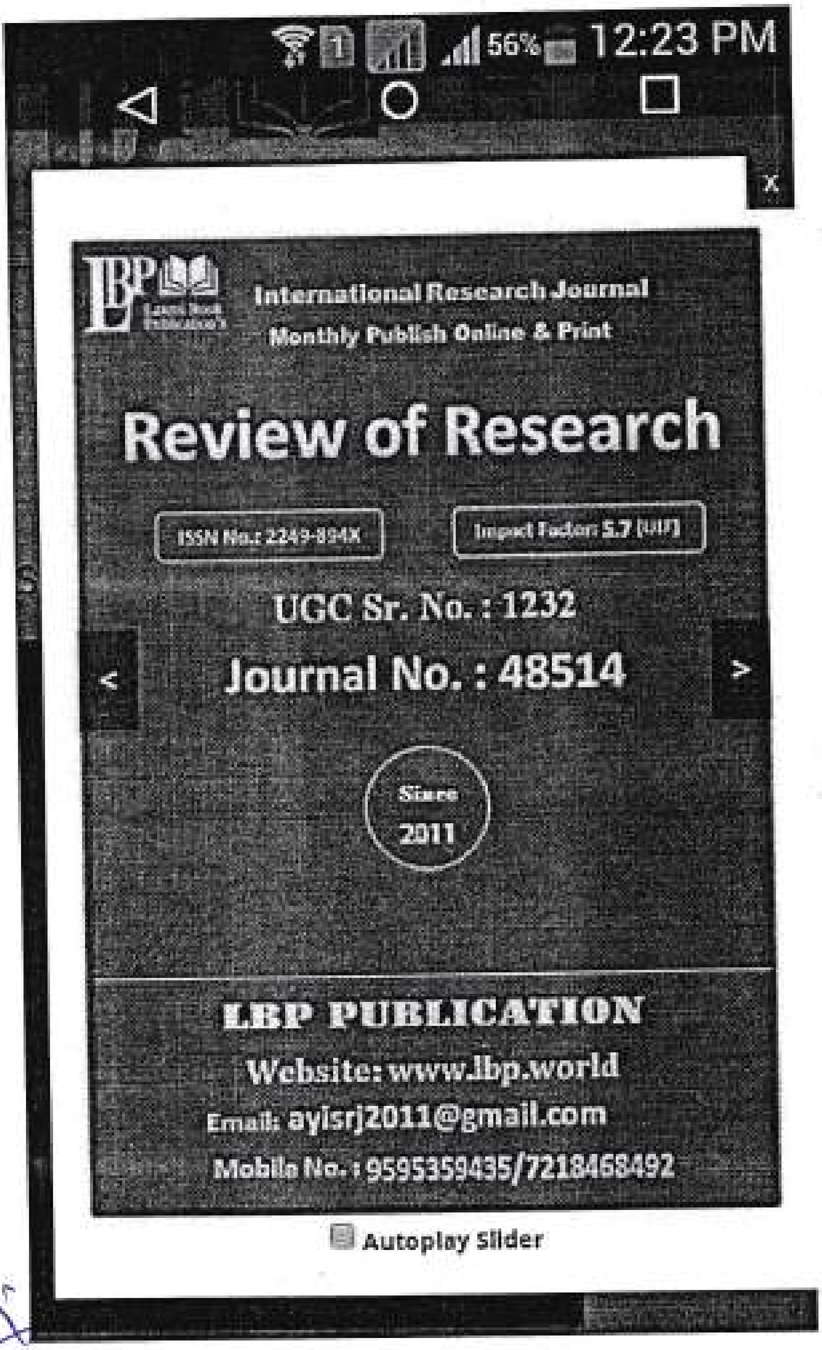

International Research Journal
Monthly Publish Online & Print

Review of Research

ISSN No.: 2249-894X

Impact Factor: 5.7 (UIF)

UGC Sr. No. : 1232

Journal No. : 48514

Since
2011

LBP PUBLICATION
Website: www.lbp.world
Email: ayisrj2011@gmail.com
Mobile No. : 9595359435/7218468492

☐ Autoplay Slider

Co-ordinator
IQAC
Shri Guru Buddhiswami Mahavidyalaya
Purna (Jn) Dist. Parbhani - 431511 (M.S.)

Estd. 1993

PRINCIPAL
Shri Guru Buddhiswami Mahavidyalaya
Purna (Jn.) Dist.Parbhani

TACS/Conf/NCRAN2019/

ertificate

Establishment -1993

Shri Gajanan Shikshan Prasarak Mandal, Yeldari Camp
(Linguistic (Marwadi) Minority Institute)
Re-accredited by NAAC with 'B' Grade

Toshniwal Arts, Commerce & Science College

Sengaon Dist. Hingoli-431542 (MS)

DEPARTMENT OF PHYSICS

Organized

National Conference

Recent Advances in Nanotechnology (RAN-2019)

This is to certify that, Dr. / Mr. / Mrs. / Ms. *S. B. Shete* of *Department of Physics S.G.B.College ,Purna* has participated in the National Conference on *"Recent Advances In Nanotechnology-2019 - An Interdisciplinary Approach"* organized by the Department of Physics, Toshniwal ACS College, Sengaon, Dist. Hingoli, (MS), India on **05th March 2019** presented (**Oral/Poster**) research work entitled *"Post Synthesis modification of Rice Husk Ash RHA-SBA-16 by Aluminum and Titanium Metal Ions"*.

Dr. R. A. Joshi
Convener

Co-ordinator
IQAC
Shri Guru Buddhiswami Mahavidyalaya
Purna (Jn) Dist. Parbhani - 431511 (M.S.)

Estd.1983

PRINCIPAL
Shri Guru Buddhiswami Mahavidyalaya
Purna (Jn.) Dist.Parbhani

Talnikar
Shri. S. G. Talnikar
Principal

REVIEW OF RESEARCH
IMPACT FACTOR : 5.7631(UIF)
ISSN: 2249-894X
VOLUME - 1 | ISSUE - 2 | MARCH - 2019

POST SYNTHESIS MODIFICATION OF RICE HUSK ASH RHA-SBA-16 BY ALUMINUM AND TITANIUM METAL IONS

Shete S. B.[1] and **Kapure G. P.**[2]
[1,2]Department of Physics S.G.B.College ,Purna,
Email: s.bshete@resdiffmail.com

ABSTRACT :

Spherical particles of mesoporous silica SBA-16 with cubic Im3m structure were synthesized at low pH using Pluronic F127 as template and RHA as silica source. The diameter of the spherical particles can be controlled in the range of 0.5–8 μm by varying Spherical particles of mesoporous silica SBA-16 with cubic Im3m structure were synthesized at low pH using Pluronic F127 as template and RHA as silica source. It is suggested that this morphology transition is due to a change in hydrolysis and condensation rate of the silica source and as a result the assembly of F127 micelles will differ. The SBA-16 samples were characterized using powder X-ray diffraction (XRD), scanning electron microscopy (SEM), transmission electron microscopy (TEM) and Nitrogen adsorption techniques.

KEYWORDS: *SBA-16; Spherical particles; Synthesis temperature; Morphology; Pluronic F127.*

INTRODUCTION:

Spherical particles of mesoporous silica SBA-16 with cubic Im3m structure were synthesized at low pH using Pluronic F127 as template and RHA as silica source. The diameter of the spherical particles can be controlled in the range of 0.5–8 μm by varying[1] .The synthesis of mesoporous materials by a liquid-crystal template mechanism was reported The properties of these materials make them attractive for adsorption, catalysis, separation, chemical sensing, optical coating, drug delivery and electronic applications. For practical purposes, the overall morphology of a mesoporous material is a necessary requirement in combination with their internal structure. SBA-16 is a mesoporous material with 3D cubic pore arrangement corresponding to Im3m space group In this body-centred-cubic structure each mesoporous is connected with its eight nearest neighbours to form a multidirectional system of mesoporous network[2-4]Due to its large cage, high surface area and high thermal stability. This material appears to be one of the best candidates for catalytic support and packing materials for separation. Using F127 as a surfactant is the common way of synthesizing SBA-16.However, there are also reports on alternative surfactants such as F108,a blend of P123 and F127[5-8].

Micro porous zeolite are widely used as solid acid catalysts, but their applications are intrinsically limited by drawback of zeolite is that the small size of the channels (less than 0.8 nm) and cavities (<1.5 nm) imposes diffusion limitations on reactions that can cause high back pressure on flow systems. The dimensions of the zeolite micro pores (< 2 nm), mesoporous (2-50nm) and macro pores (> 50 nm) permit faster migration of guest molecules in the host frameworks. Since fast mass transfer of the reactants and products to and from the active sites is required for catalysts[9-11],the concept of infusing mesoporous into zeolite particles has attracted much attention. Recent progress involving this issued to ordered mesoporous materials such as MCM-41, SBA-16 and SBA-15[12-16]. These mesoporous materials have pore diameters of 3.0 nm– 8.0nm and exhibit catalytic properties for the catalytic conversion of bulky reactants, but unfortunately, when compared with micro porous zeolite[17-18],the catalytic activity and hydrothermal stability are relatively low, which can be attributed to the amorphous nature of the mesoporous walls. To overcome this problem, some recent research efforts have been concentrated on introducing mesoporous or macro pores linked to the zeolite micro pores.

These materials called Hierarchical zeolite materials with combinations of micro/meso/macro pores would further extend the application of zeolite as solid acid[19].

POST MODIFICATION OF RHA-SBA-16 BY Al^{++} and Ti^{++}:

So as to impart the catalytic and adsorptive activity to the chemically inert mesoporous silicate framework, substitution of Si^{4+} ions by other heteroatom in the prepared materials has been endeavored. This part describes the synthesis procedures used for post modification of RHA-SBA-16 by introducing heteroatoms such as Aluminum and Titanium into their meso-structures to improve their catalytic activity of reactions of bulky molecules and the adsorption activity significantly[20-22]. The post modification synthesis of RHA-SBA-16 can be possible by various methodologies; among them we have followed the ion exchange method.In this method, the presence of Aluminum in the silica alumina mesoporous framework gives rise to anion, which attracts cations in the framework as they are loosely bounded. The replacement of cation held in the framework structure is possible by the ion present in the external solution. Hence ion exchange is possible[23]. Initially RHA-SBA-16 was converted in to their protonic forms. The 100% crystalline RHA-SBA-16 sample in its protonic form was selected and was further modified by using batch ion exchange method with metal ions like Al^{+++} and Ti^{++} with different metal ion concentrations. Introduction of metal ions such as Al, and Ti, creates new Lewis acid sites and Bronsted basic sites respectively within the RHA-SBA-16 host.

EXPERIMENTAL:

Post Synthesis Modification of RHA-SBA-16 with H^+:

Exchange of RHA-SBA-16 in to its protonic form was done by batch ion exchange method using subsequent acidic salt solutions. Ammonium nitrate 2.5wt % (2g) was taken in a 150 ml single neck round bottomed flask and 25 ml methanol was added into it as a solvent.

10g of the dried RHA-SBA-16 powder was also added and the blend was stirred under reflux condition for 3h at 80°C. Then this mixture was allowed to cool to room temperature by natural convection followed by filtration. Further the filtrate was washed repeatedly with deionized water.The residue is NH_4-RHA-SBA-16. It is dried for overnight by heating at 100°C in an oven. Later on, NH_4-RHA-SBA-16 is heated at 500°C in automated muffle furnace for 3h, to exile ammonia and is converted in H^+ form i.e.H-RHA-SBA-16.

Post Synthesis Modification of H-RHA-SBA-16 by Al^{+++} metal ions:

To tune and enhance the acidic behavior of RHA-SBA-16, we have exchanged its protonic form into modified Al-RHA-SBA-16 using corresponding metal salt solutions of different molarities by ion exchange method as described earlier. The calculated quantity of concentrated salt solution of Al^{+++} [Al2(SO4)3.18 H2O] i.e.10.28g for 1M, 8.23g for 0.8M and 5.15g for 0.5M in 30g of methanol were taken in three different single neck round bottom flask (RBF) of 150 ml. Then 5g of the dried H-RHA-SBA-16 powder was added to it and was stirred under reflux condition for 6h at 100°C. Later the mixture was brought to room temperature naturally and then the solvent was evaporated. The residue was dried in the oven at 100°C, and calcined at 450°C to500°C for 4h.To ensure the ion exchange of the Al^{+++} in RHA-SBA-16 we have examined the elemental composition of the calcined samples by EDAX and came to know that their Si/Al ratio varies from 4-9. These modified forms were named as Al-RHA-SBA-16 (Si/Al = 4, 7 and 9).

Post Synthesis Modification of H-RHA-SBA-16 by Ti^{++} metal ions:

To tune and enhance the basic behavior of RHA-SBA-16, we have exchanged its protonic form into modified Ti-RHA-SBA-16 using corresponding metal salt solutions of different molarities by ion exchange method as described earlier. The calculated quantity of concentrated salt solution of TiO_2i.e.0.8g for 2wt%, 1.3g for 4wt%and 1.9g for 6wt% in 30g of methanol were taken in three different single neck round bottom flask (RBF) of 150 ml. Then 5g of the dried H-RHA-SBA-16 powder was added to it and was stirred under reflux condition for 6h at 90°C. Later the mixture was brought to room temperature naturally and later the solvent was evaporated. The residue was dried in the oven at 100°C, and calcined at 450°C to500°C for 4h.To ensure the ion exchange of the Ti^{++}in RHA-SBA-16 we have examined the elemental composition of the calcined samples by EDAX. These modified forms were named as Ti-RHA-SBA-16 (2wt%, 4wt% and 6wt%).

RESULTS AND DISCUSSION:

Energy Dispersive Analysis of X-ray (EDAX):

Table 1 Elemental Composition of the Samples Analyzed by EDAX

Sample name	Si	Al	Si/Al ratio	Ti Metal ion wt%
Al-RHA-SBA-16 (Si/Al=4)	56.81	14.68	Si/Al=3.87 ≈ 4	–
Al-RHA-SBA-16 (Si/Al=7)	64.62	9.42	Si/Al=6.86 ≈7	–
Al-RHA-SBA-16 (Si/Al=9)	69.30	7.83	Si/Al=8.85 ≈9	–
Ti-RHA-SBA-16 (2wt %)	68.47	1.74	–	Ti =1.91 ≈2
Ti-RHA-SBA-16 (4wt %)	63.71	1.78	–	Ti =3.83 ≈4
Ti-RHA-SBA-16 (6wt %)	64.11	1.81	–	Ti =5.76 ≈6

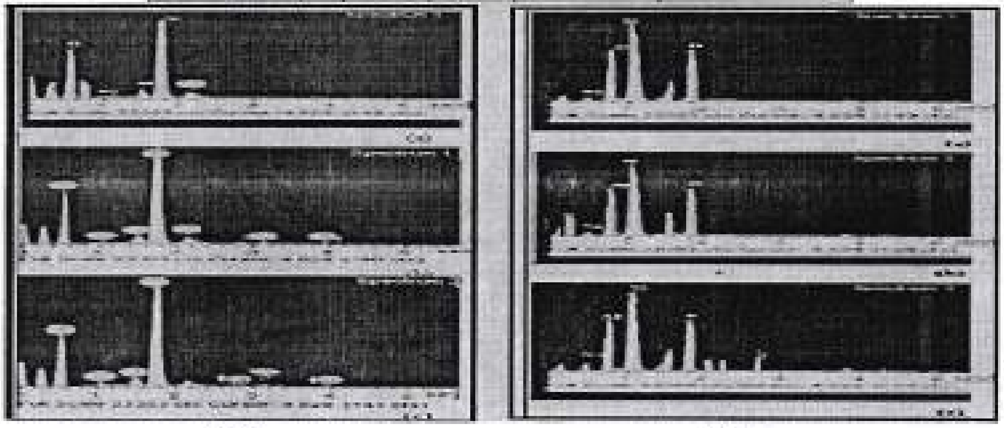

(A) (B)

Fig.1. (A) EDAX IMAGES OF (a) Al-RHA-SBA-16(Si/Al=5), (b) Al-RHA-SBA-16(Si/Al=9) and (c) Al-RHA-SBA-16(Si/Al=11).

(B) EDAX IMAGES OF (a)Ti-RHA-SBA-16 (2wt %), (b) Ti-RHA-SBA-16 (4wt %) and (c) Ti-RHA-SBA-16 (6wt %).

The observed EDAX spectra for all the modified samples analyzed are shown in Fig. 1.(A, B). In EDAX, X-ray photons emitted from the sample are dispersed by a crystal and plotted as a function of energy. The X-rays being analyzed came from the area being imaged, so elemental composition is determined as a function of location on the sample. Outstandingly it is observed that the atomic percentage of Si, Al, Ti and O in modified forms of the RHA-SBA-16 are almost uniform. Even the Si/Al ratio is observed to be within the range in case of modified RHA-SBA-16 which shows that, the elementary compositions in the modified samples are uniform. The observations made by using SEM-EDAX correlate well with the XRD data for all the analyzed samples. The amount of Ti- metal ions weight percentage in all the samples is found to be around 1.93–5.71wt%. The metal compositions after the modification with the RHA-SBA-16 samples are given in Table 1.

calcined samples by EDAX. These modified forms were named as Ti-RHA-SBA-16 (2wt%, 4wt% and 6wt%).

RESULTS AND DISCUSSION:

Energy Dispersive Analysis of X-ray (EDAX):

Table 1 Elemental Composition of the Samples Analyzed by EDAX

Sample name	Si	Al	Si/Al ratio	Ti Metal ion wt%
Al-RHA-SBA-16 (Si/Al=4)	56.81	14.68	Si/Al=3.87 ≈ 4	–
Al-RHA-SBA-16 (Si/Al=7)	64.62	9.42	Si/Al=6.86 ≈7	–
Al-RHA-SBA-16 (Si/Al=9)	69.30	7.83	Si/Al=8.85 ≈9	–
Ti-RHA-SBA-16 (2wt %)	68.47	1.74	–	Ti =1.91 ≈2
Ti-RHA-SBA-16 (4wt %)	63.71	1.78	–	Ti =3.83 ≈4
Ti-RHA-SBA-16 (6wt %)	64.11	1.81	–	Ti =5.76 ≈6

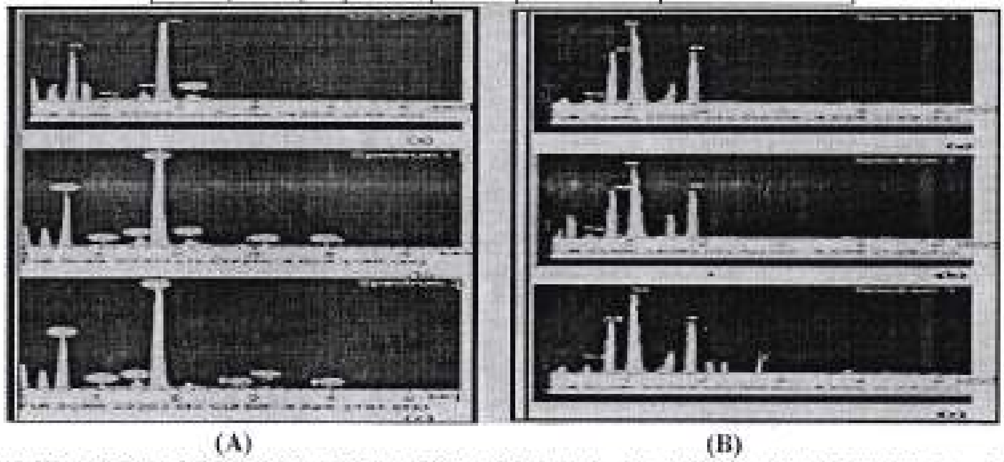
(A) (B)

Fig.1. (A) EDAX IMAGES OF (a) Al-RHA-SBA-16(Si/Al=5), (b) Al-RHA-SBA-16(Si/Al=9) and (c) Al-RHA-SBA-16(Si/Al=11).

(B) EDAX IMAGES OF (a)Ti-RHA-SBA-16 (2wt %), (b) Ti-RHA-SBA-16 (4wt %) and (c) Ti-RHA-SBA-16 (6wt %).

The observed EDAX spectra for all the modified samples analyzed are shown in Fig. 1.(A, B). In EDAX, X-ray photons emitted from the sample are dispersed by a crystal and plotted as a function of energy. The X-rays being analyzed came from the area being imaged, so elemental composition is determined as a function of location on the sample. Outstandingly it is observed that the atomic percentage of Si, Al, Ti and O in modified forms of the RHA-SBA-16 are almost uniform. Even the Si/Al ratio is observed to be within the range in case of modified RHA-SBA-16 which shows that, the elementary compositions in the modified samples are uniform. The observations made by using SEM-EDAX correlate well with the XRD data for all the analyzed samples. The amount of Ti- metal ions weight percentage in all the samples is found to be around 1.93–5.71wt%. The metal compositions after the modification with the RHA-SBA-16 samples are given in Table 1.

X-ray diffraction (H-RHA-SBA-16, Al-RHA-SBA-16, Ti-RHA-SBA-16)

This section gives detailed information on characterization data of the H-RHA-SBA-16, Al-RHA-SBA-16 and Ti-RHA-SBA-16 samples with different Si/Al ratios and with different wt.% of Ti- exchanged respectively.The XRD patterns of the calcined parent H-RHA-SBA-16 Al-RHA-SBA-16 and Ti-RHA-SBA-16 samples with different Si/Al ratios (4, 7 and 9) and with different wt.% of Ti (2wt.%, 4wt.% and 6wt.%) respectively are presented in Fig. 2 (A, B, C) respectively. The spectra showed XRD patterns identical to that reported for standard SBA-16 materials. Becker *al.* indexed these peaks for a hexagonal unit cell, the parameter of which was calculated from the equation $a_0 = \sqrt{2}d_{110}$.

On calcination of samples, the peak is shifted to lower d_{110} spacing value probably due to condensation of internal Si-OH groups giving rise to a contraction of the unit cell. The unit cell parameter and d-spacing of the Al-RHA-SBA-16, Ti-RHA-SBA-16 samples and H-RHA-SBA-16 are given in Table 2. The slight increase in d-spacing and unit cell parameters of both Al-RHA-SBA-16 and Ti-RHA-SBA-16 compared to H-RHA-SBA-16 suggests the presence of Aluminum and Titanium in the framework respectively. The increase in unit cell parameter on Al or Ti incorporation is probably due to the replacement of shorter Si-O bonds by longer Al-O and Ti-O bonds in the structure respectively. It is also observed that along with an increase in the unit cell parameter, the (110) diffraction peak becomes broader and less intense with increasing Aluminum or Titanium content, probably because of the change of the Al-O-Al and Ti-O-Ti bond angle, causing a distortion in the long range ordering of the hexagonal mesoporous structure.

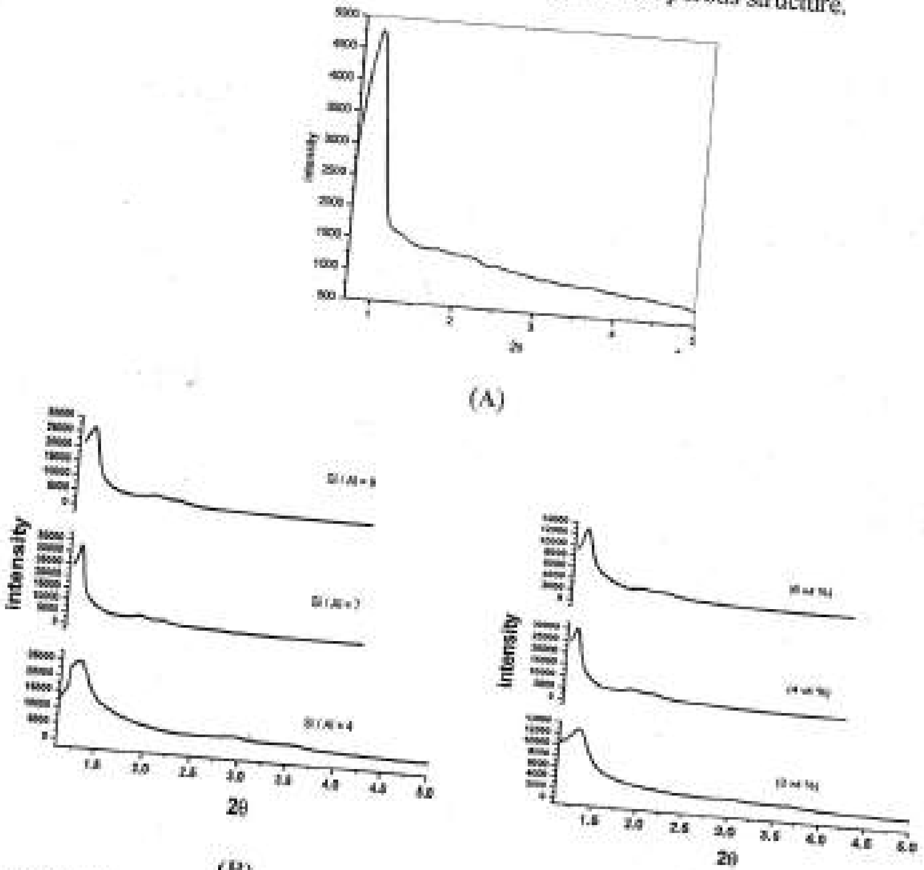

(A)

(B)

(C)

Fig. 2 A) XRD patterns of calcined parent H-RHA-SBA-16sample. B)Al-RHA-SBA-16 (i.e. Si/Al=4, 7, 9) C) Ti-RHA-SBA-16 (i.e.2wt.%, 4wt.% and 6wt.%)

Fig. 2. (B, C) illustrate that in all the modified forms of H-RHA-SBA-16 sample, there are marginal changes in the crystallinity but almost no changes in the phase purity and structural morphology are being observed after modification with different amounts of $Al^{+++}$and Ti^{++} percentage. This indicates the structural stability of the parent sample and presence of metal ions in the intra-crystalline voids of the H-RHA-SBA-16. The percent crystallinity of the samples is drawn with the amount of metal ion percent in them. From the Table 2.as the metal ions percent increases in modification, an increase in the crystallinity of the samples was observed up to Si/Al=4 and 6wt% of Ti. But when Si/Al > 4 and Ti incorporation is more than 6wt% i.e. when the metal ion concentration increases then the sample declines from good crystallinity to amorphous nature. This is because of the fact that, Al itself is having an amorphous nature and Ti being strong earth metal it produces other amalgamations in the structure influencing the crystallinity, hence the modification was stopped after Si/Al=4 and more than 6wt% of Ti incorporation to retain the crystallinity of the sample. The crystallinity of the sample was 100% for H-RHA-SBA-16.If the 'Al' metal ion concentration in H-RHA-SBA-16 was Si/Al = 4 crystallinity was 98.5% and then gradually decreased for Si/Al=7, 9 as 91.3% and 86.5% respectively. However, if the 'Ti' metal ion concentration in H-RHA-SBA-16 was 6wt%, it was 96.5% and then gradually decreased for 4wt% and 2wt% as 84.3% and 80.4% respectively.

Fig. 3.depicts the co-relation between % crystallinity and concentration of Al and Ti metal ions.

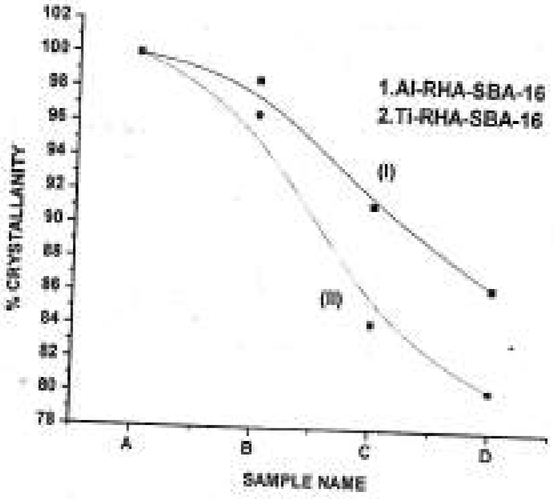

Fig.3 Effect of the metal concentration on Percent CrystallinityofH-RHA-SBA-16

Furthermore, XRD patterns recorded at higher angles up to 80° showed no peaks. Therefore, the presence of any crystalline Al or Ti containing species can be excluded.

Table 2 Physicochemical properties of Al-RHA-SBA-16 and Ti-RHA-SBA-16 samples

Sample	d_{110}	Surface Area(m^2/g)	Pore Volume (ml/g)	Pore diameter(A^0)	% Crystallanity	Acidity (mmole/g)
H-RHA-SBA-16	33.16	954.22	0.65	27.3	100	0.014
Al-RHA-SBA-16 (Si/Al=4)	33.32	852.00	0.76	28.6	98.5	0.192
Al-RHA-SBA-16 (Si/Al=7)	34.62	826.46	0.71	31.2	91.3	0.086
Al-RHA-SBA-16 (Si/Al=9)	35.75	938.61	0.69	26.8	86.5	0.044

Ti-RHA-SBA-16 (2wt%)	45.56	789.36	0.62	30.9	80.4	0.017
Ti-RHA-SBA-16 (4wt%)	45.85	809.58	0.68	30.4	84.3	0.019
Ti-RHA-SBA-16 (6wt%)	45.58	926.25	0.72	29.8	96.5	0.024

Sorption studies:

The BET surface areas, average pore diameters and pore volumes calculated from N_2-sorption isotherms of Al-RHA-SBA-16 (Si /Al = 4, 7, 9) and Ti-RHA-SBA-16 (2wt%, 4wt%, 6wt%) presented in Table 2. According to IUPAC classification, the isotherms are of type IV[68] presented for Al-RHA-SBA-16 (Si /Al = 4, 7, 9) and Ti-RHA-SBA-16 (2wt%, 4wt%, 6wt%) in Fig. 4. (A, B) and 5.(A, B) respectively.

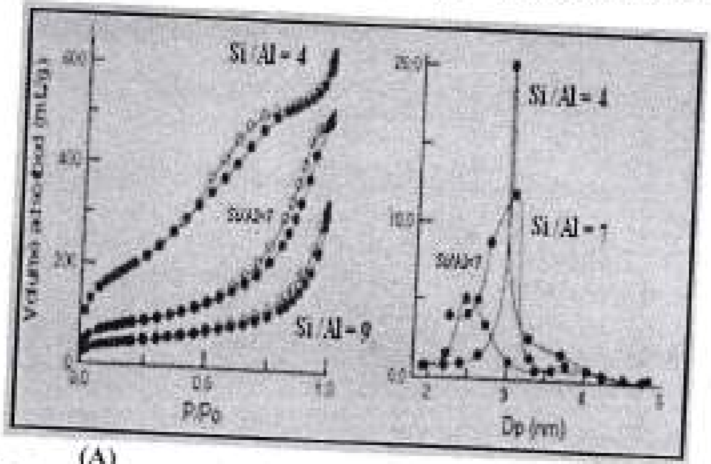

(A)

(B)

Fig. 4.A) N_2-adsorption-desorption isotherms and (B) Pore size distribution of Al-RHA-SBA-16(Si /Al = 4, 7, 9)

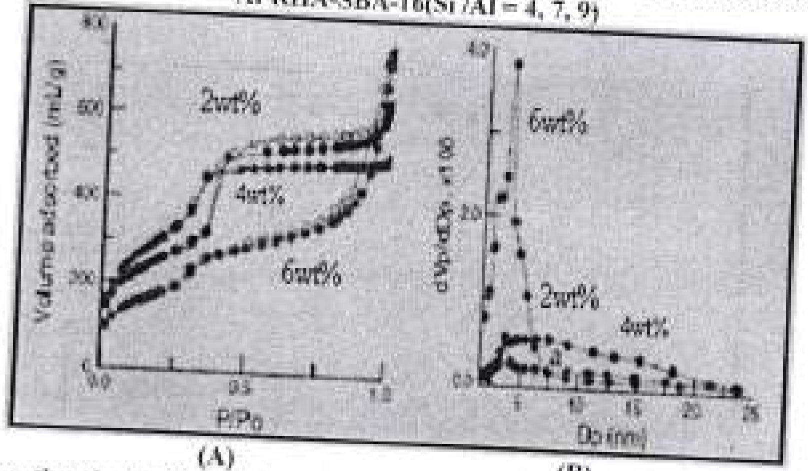

(A)

(B)

Fig. 5.A) N_2-adsorption-desorption isotherms and (B) Pore size distribution of Ti-RHA-SBA-16(2wt%, 4wt%, 6wt%)

The position of p/p_0 at which inflection starts is related to the diameter of the mesopores. The sharpness in this step indicates the uniformity of the pore size distribution. In the case of both M-RHA-SBA-16 (M = Al or Ti), thisstep of isotherm shifts slightly towards higher relative pressure p/p_0 with increase in metal content of the sample indicating increase in the pore size. However, broadening of the hysteresis loop increases with increase in the metal content. This may be due to changes in the contour of the mesopores. The hysteresis loop in the range of $p/p_0 > 0.8$ due to capillary condensation in the inter-particle mesopores is observed in case of M-RHA-SBA-16. A comparison of the hysteresis loops of these two sets of samples at higher relative pressure region indicates difference in their textural mesoporosity. The pore diameters increase with increasing metal (Al or Ti) content of the samples.

Temperature Programmed Desorption of Ammonia

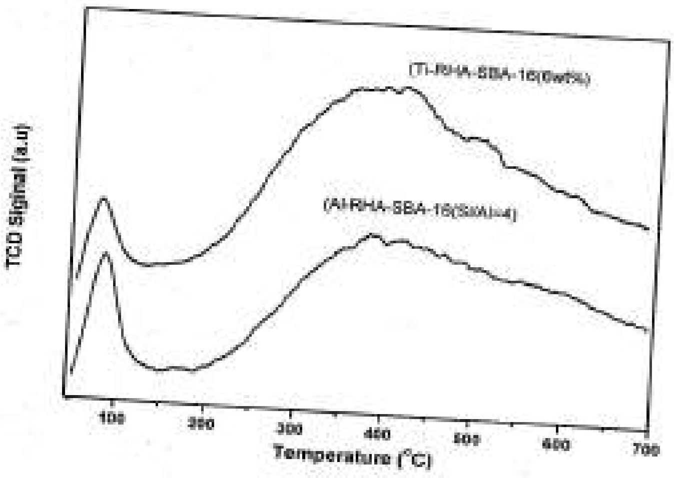

Fig.6. Temperature Programmed Desorption of Ammonia of Ti-RHA-SBA-16

The acidities of the H-Al-SBA-16 samples were characterized by the TPD of Ammonia. The acid strengths appear to be rather moderate as nearly all the Ammonia desorbed below 250°C. The acidities (mmol/g) based on the Ammonia desorbed by the samples beyond 90°C are presented in Table 2.

As the Aluminum content increases, the total acidity increases in the samples (Al-RHA-SBA-16(Si/Al=9) <Al-RHA-SBA-16(Si/Al=7) <Al-RHA-SBA-16 (Si/Al=4). However as the Titanium content increases, the total acidity decreases in the samples (Ti-RHA-SBA-16 (2wt%)< Ti-RHA-SBA-16 (4wt%) < Ti-RHA-SBA-16 (6wt %)).

SEM

(Si/Al=4) (Si/Al=7) (Si/Al=9)

Fig. 7.Scanning electron micrograph of Al-RHA-SBA-16.

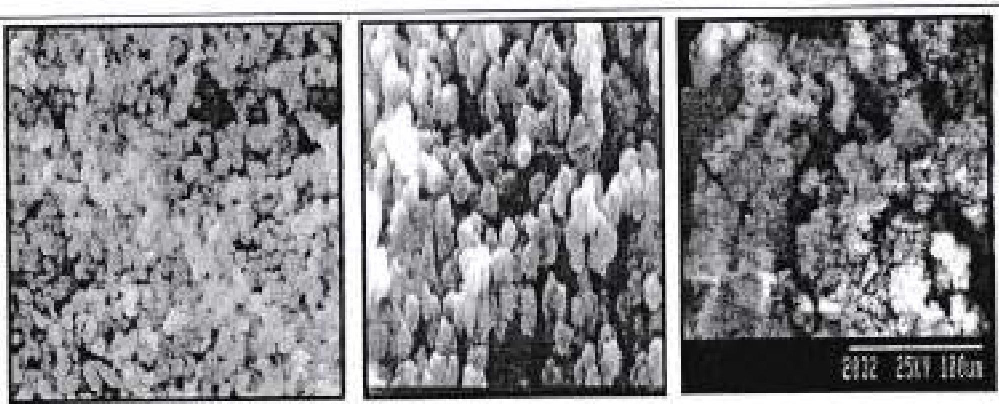

(2wt%) (4wt%) (6wt%)

Fig. 8. Scanning electron micrograph of Ti-RHA-SBA-16.

Scanning electron micrographs of all the modified Al-RHA-SBA-16 (Si/Al=4, 7, 9) and Ti-RHA-SBA-16 (2, 4, 6wt %) samples is presented in Fig. 7.and Fig. 8.respectively. The micrographs reveal two morphologies, such as hexagonal and spherical habit and majority of them are hexagonal shaped agglomerates of small particles of the size between 3.10–10.60A^0.It is seen that the morphology of the crystals gets affected as the metal ion percent gradually increased. The SEM photograph of H-RHA-SBA-16 sample shows bigger crystal size while the modified forms the metal ions have decreased crystal size which may affect the surface properties of the H-RHA-SBA-16 which tend to use it for different applications.

FTIR

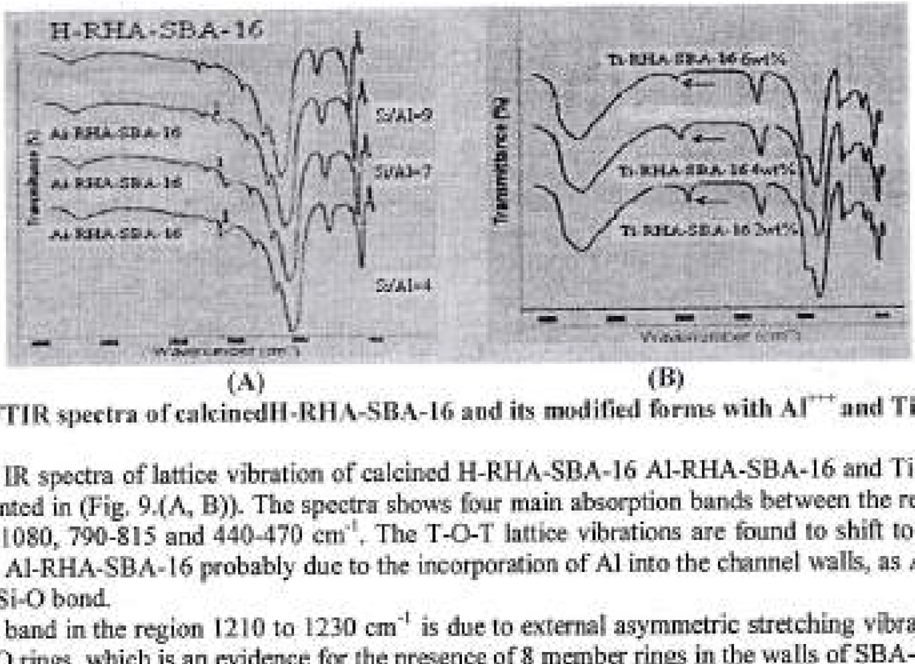

(A) (B)

Fig.9.FTIR spectra of calcinedH-RHA-SBA-16 and its modified forms with Al^{+++} and Ti^{++} ions.

The IR spectra of lattice vibration of calcined H-RHA-SBA-16 Al-RHA-SBA-16 and Ti-RHA-SBA-16 are presented in (Fig. 9.(A, B)). The spectra shows four main absorption bands between the regions 1210-1230, 1045-1080, 790-815 and 440-470 cm^{-1}. The T-O-T lattice vibrations are found to shift to lower wave numbers for Al-RHA-SBA-16 probably due to the incorporation of Al into the channel walls, as Al-O bond is longer than Si-O bond.

The band in the region 1210 to 1230 cm^{-1} is due to external asymmetric stretching vibrations of five member Si-O rings, which is an evidence for the presence of 8 member rings in the walls of SBA-16 structure. This band becomes less intense in the calcined samples indicating probably a rearrangement of the wall structure due to high temperature treatment.

The band in the region 1045-1090 cm^{-1}due to internal asymmetric stretching mode of SiO_4(TO_4) skeleton appears to be the strongest band in the spectra of all silicates. The broadening of this band on calcination may be due to superimposition of many bands ascribable to TO_4 arising from different T-O-T angles, this band is significantly shifted to a lower wave number (1066cm^{-1}). This may be due to the stretching of Si-O bond by long chain surfactant molecules forming micelles around which the SiO4 species are wound during formation of the mesoporous molecular sieves. Interestingly, this band at~ 1066 cm^{-1} of mesoporous molecular sieves is found to be shifted to the higher wave number i.e.~1085 cm^{-1} on removal of the surfactant molecules during calcination. This suggests that contraction of Si-O bond takes place during calcination, which has also been confirmed by XRD characterization.All IR spectra exhibit one common feature, a band at ~970 cm^{-1}. The correct interpretation of this vibrational band has been a matter of extensive studies. Fig.9. shows that within corporation of metal ions, the intensity of this band marginally increases. This band is generally considered as a proof for the incorporation of the heteroatom into the framework.

REFERENCES:

1. G. Ferraiolo, M. Zilli, A. Converti, Fly ash disposal and utilization, *J. Chem. Technol. Biotechnol.*47, 281–305, **(1990)**.

2. C.L. Carlson, D.C. Adriano, Environmental impact of coal combustion residue, *J. Environ. Qual.* 22, 227–247, **(1993)**.

3.. KekaOza, Narayan C Pradhan; AmarnathSamanta*Bull Matter science.*,Vol.27 pp 555-564, **(2004)**.

4.. Coal Resources of India S. Farooq Department of Geology AMU.

5.. Adler KB, Mossman BT, Butler GB, Jean LM, Craighead JE Interaction of Mount St. Helens' volcanic ash with cells of the respiratory epithelium. *Environ Res* 35:346–361, **(1984)**.

6. Akematsu T, Dodson RF, Williams MG, Hurst GA, The short-term effects of volcanic ash on the small airways of the respiratory system. *Environ Res* 29:358–370, **(1982)**.

7. Baxter PJ The eruption of El Reventador volcano 2002: health hazards and the implications for volcano risk management in Ecuador. Report to the *Pan-American Health Organization, Pan American Health Organization, Washington DC*(**2003**).

8. Baxter PJ, Ing R, Falk F, French J, Stein GF, Bernstein RS, Merchant JA, Allard J Mount St Helens eruptions, May 18 to June 12 1980. *J Am Med Assoc* 246: 2585–2589, **(1981)**.

9. Baxter PJ, Woo G, Pomonis A Preliminary assessment of volcanic risk on Montserrat.*Montserrat Volcano Observatory, Montserrat*, p 32, **(1998)**.

10. Baxter PJ, Bonadonna C, Dupree R, Hards VL, Kohn SC, Murphy MD, Nichols A, Nicholson RA, Norton G, Searl A, Sparks RSJ, Vickers BP Cristobalite in volcanic ash of the *Soufrière Hills Volcano, Montserrat, British West Indies. Science* 283:1142–1145, **(1999)**.

11. FAO Food Outlook, *Food and Agriculture Organization of the United Nations*, November, **(2011)**.

12. ERIKSON, S. and PRIOR, M., *"The Briquetting of Agricultural Waste for Fuel"*, FAO Environment and Energy paper 11, FAO of the UN, Rome. **(1990)**.

13. Corma, *A. Chem. Rev.* 95, 559-614, **(1995)**.

14. Mirodatos, C.; Barthomeuf, D. *J. Catal.*93, 246, **(1985)**.

15. Wilson, S. T.; Lok, B. M.; Flanigen, E. M. *U.S. Patent* 4,310,440, **(1982)**.

16. Dessau, R. M.; Schlenker, J. L.; Aiggins, *J. B. Zeolites*, 10, 522, **(1990)**.

17. Kresge, C. T.; Leonowicz, M. E.; Roth, W. J.; Vartulli, J. C.; Beck, J. S. *Nature* 359, 710, **(1992)**.

18. Beck, J. S.; Chu, C. T.; Johnson, I. D.; Kresge, C. T.; Leonowicz, M. E.; Roth, W. J.; Vartulli, J. C. U.S. Patent 5,108,725, **(1992)**.

19. Beck, J. S.; Calabro, D. C.; McCullen, S. B.; Pelrine, B. P.; Schmitt, K. D.; Vartulli, J. C. *U. S. Patent* 5, 145, 816, **(1992)**.

20. Beck, J. S.; Kresge, C. T.; Leonowicz, M. E.; Roth, W. J.; Vartulli, J. C. *U.S. Patent* 5, 264, 203, **(1993)**.

21. Beck, J. S.; Smith, K. D.; Vartulli, J. C. U.S. Patent 5,334,368, 1994. Beck, J. S.; Kresge, C. T.; McCullen, S. B.; Roth, W. J.; Vartulli, J. C. *U.S. Patent* 5,370,785, **(1994)**.

22. Beck, J. S.; Vartulli, J. C.; Roth, W. J.; Leonowicz, M. E.; Kresge, C. T.; Schmitt, K. D.; Chu, C. T.-W.; Olson, D. H.; Sheppard, E. W.; Mc Cullen, S. B.; Higgins, J. B.; Schlenker, J. L. *J. Am. Chem. Soc.*, 114, 10834, **(1992)**.

23. W.M. Meier, "Zeolite Structure" *Molecular Sieves*, Society for Chemical Industry, London, p. 10-25, **(1968)**.